N87-17613

THE SINGLE SCATTERING PHASE FUNCTIONS OF JUPITER'S CLOUDS

L. R. Doose, M. G. Tomasko, and N. D. Castillo
Lunar and Planetary Lab., University of Arizona

The determination of the single scattering phase functions of Jupiter's clouds and a thin upper haze by Tomasko et al. (1978, Icarus 33, 558-592) has been refined and extended to seven latitudes in blue and red light. The phase function is well-constrained by the Pioneer 10 and 11 photometric data sets. Multiple scattering models were computed to match the limb darkening at each latitude at up to 15 phase angles from 12° to 151°. Ground-based observations were used for absolute calibration and to extend the data to lower phase angles. The phase functions were parameterized using the double Henyey-Greenstein function. The three Henyey-Greenstein parameters and the single scattering albedo were determined using a non-linear least squares method for the haze and the clouds below. The phase functions derived for the northern zone and belt are remarkably similar to the phase functions of the corresponding regions in the south, with most of the differences in brightness of the northern and southern features resulting from minor differences in single scattering albedo. Analysis of the Equatorial Region is complicated by the presence of numerous small features, but the phase function required is generally similar to that seen in the more homogeneous regions. Details of the phase functions of the haze and clouds are presented, and the differences between the cloud phase functions at low and high latitudes in red and blue light are discussed.

The phase function for the scattering of light by a cloud particle in Jupiter's atmosphere can serve to constrain the size, shape, and index of refraction of the particle. Atmospheric radiative transfer models which include scattering also require knowledge of the phase function. We have used photometry from Pioneers 10 and 11 covering phase angles from 12° to 151° to determine the phase function of Jupiter's clouds at seven latitudes in blue (0.44 μm) and red (0.64 μm) light. Ground-based observations from Orton (1975) made near the time of the Pioneer encounters have been included to provide data at smaller phase angles.

Figures 1 and 2 illustrate the dependence of the limb darkening of Jupiter over a range of phase angles upon the phase function. This dependence permits the solution for the phase function. Figure 1 shows the angular scattering dependence of four simple Henyey-Greenstein functions and one double Henyey-Greenstein. A Henyey-Greenstein function is described by

$$P(\Theta,g) = (1 - g^2)/(1 + g^2 - 2g\cos(\Theta)),$$

where θ is the scattering angle and g is the asymmetry parameter. A double Henyey-Greenstein is a linear combination of two such functions:

$$P(\theta) = f\ P_1(\theta,g_1) + (1 - f)\ P_2(\theta,g_2).$$

Double Henyey-Greenstein functions add the possibility of a backscattering peak to the phase function. Figure 2 compares radiative transfer models computed with the phase functions of Fig. 1 to Pioneer limb darkening data. The shape of the limb darkening at any one phase angle cannot be used to determine the phase function. Instead the limb darkening curve at each phase angle tends to constrain the single scattering phase function at the corresponding scattering angle (180°-phase angle). Observations at several phase angles are needed to choose between the phase functions of Fig. 1. Note in Fig. 2a that both the double Henyey-Greenstein and the strongest forward scattering single Henyey-Greenstein give reasonable fits. However at 12° (Fig. 2c) this single Henyey-Greenstein function results in a model which falls far below the data. The data at 34° (Fig. 2b) do not discriminate well between the phase functions. Figure 3 condenses the comparison of data at 15 phase angles on to one graph by plotting only a single data point, near the maximum brightness, for each phase angle against the models. Isotropic scattering (g = 0) fails to fit except at about 70° and 180°. The single Henyey-Greenstein with g = 0.75 fails at angles larger than about 150°. The need for a backward peak in the phase function is again illustrated.
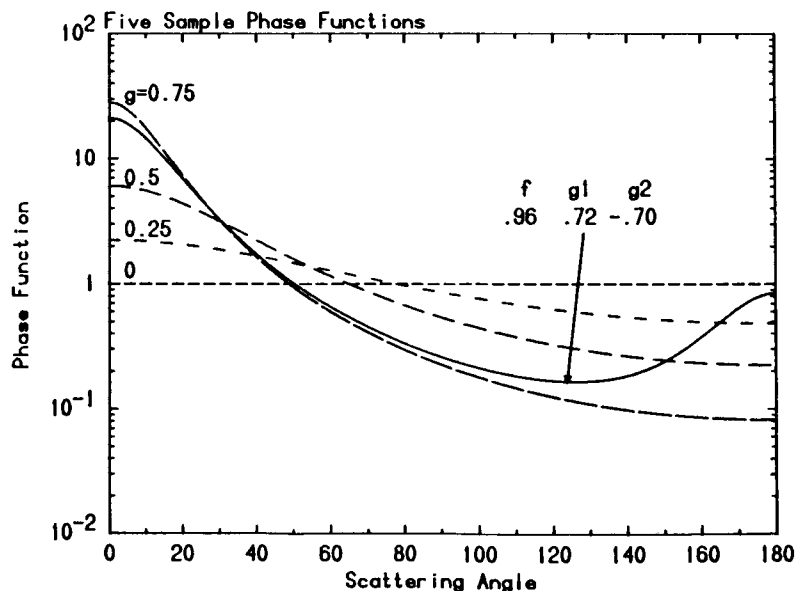

Figure 1. Angular scattering dependence for four single Henyey-Greenstein functions (labeled with asymmetry parameters at left) and one double Henyey-Greenstein function.
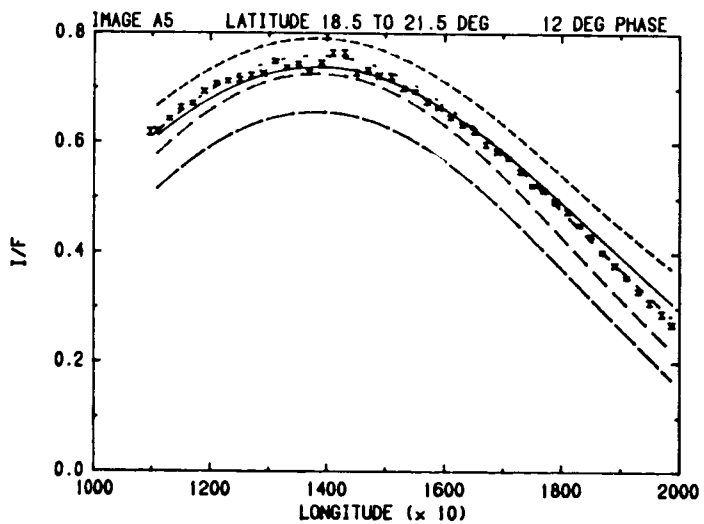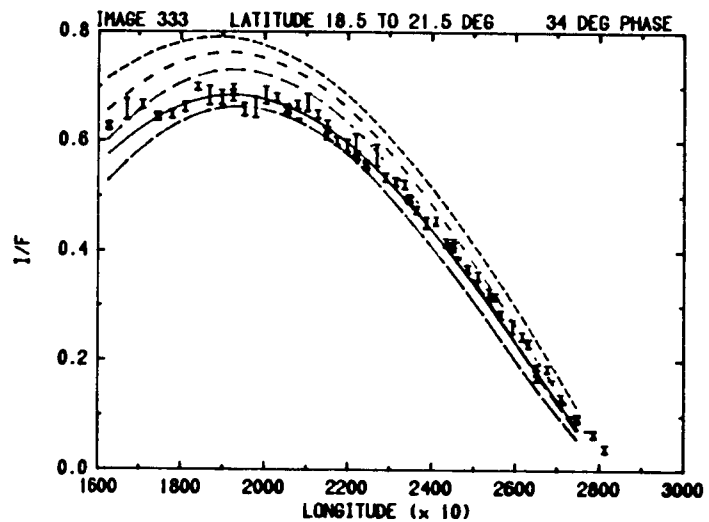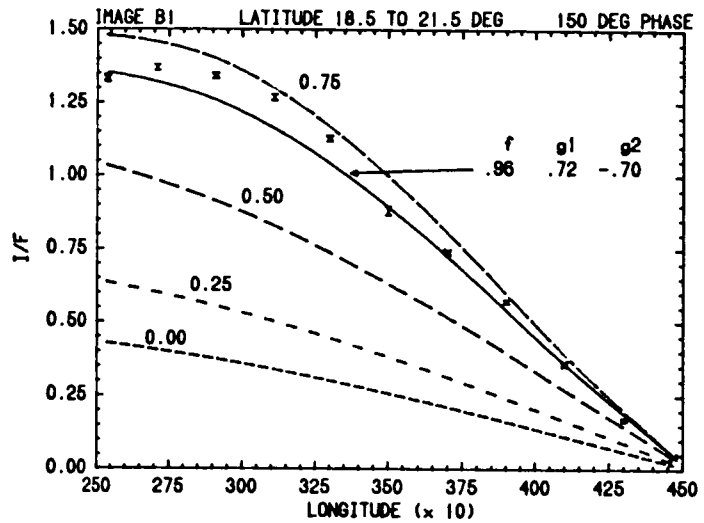
Figure 2. Limb darkening predicted by radiative transfer models using the five phase functions from Fig. 1 are compared to Pioneer photometric observations at phase angles of 150° (top), 34° (middle), and 12° (bottom). The correct phase function must yield fits at all phase angles. Only the double Henyey-Greenstein comes close. All Pioneer data available are plotted, but the best fit was determined by comparing models to a subset of points denoted with an X. Cloud features cause a fluctuation of observed limb darkening which the models cannot follow in detail.
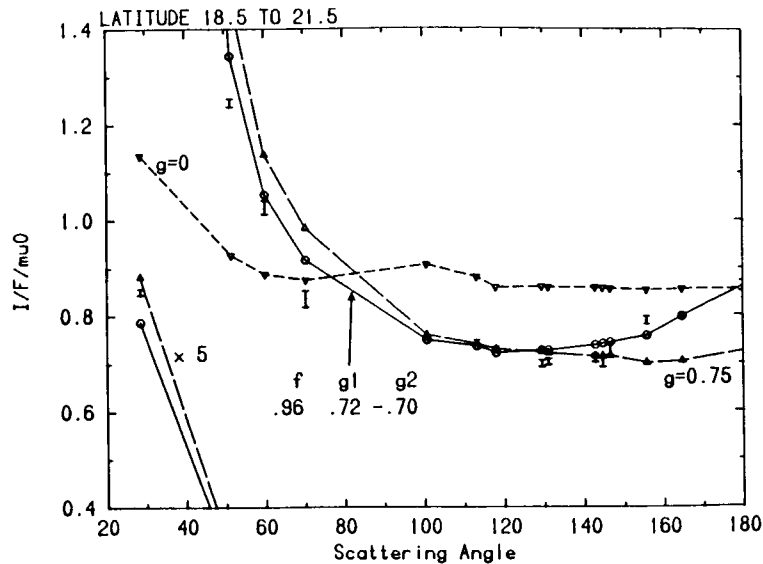
85

LATITUDE 18.5 TO 21.5

I/F/mu0

g=0

x 5

f   g1   g2
.96   .72 -.70

g=0.75

20   40   60   80   100   120   140   160   180
Scattering Angle

Figure 3. The "normalized reflectivity",
I/(μ_0F), for observed points near the maxi-
mum brightness of the limb darkening curve
at 15 phase angles plotted vs. scattering
angle. Isotropic scattering gives a poor
fit. A backscattering peak is needed to
match the small phase angle data.

We used a non-linear least-squares technique to find values for f, g_1, and g_2
and for ω, the single scattering albedo, which optimized the fit to the data
at 15 phase angles. The phase function is constrained best near the scatter-
ing angles where observations exist, as indicated by short vertical lines
near the top of each phase function plot in this paper. No observations
exist at scattering angles less than 29° (phase angles greater than 151°),
hence variations among the functions in this range are not meaningful.

The double Henyey-Greenstein functions which best fit the data are shown in
Figs. 4 through 11. Computation of radiative transfer models requires that
the vertical structure of the atmosphere, in terms of optical depth, phase
function, and single scattering albedo, be specified. We have used two
vertical structures. Structure I contains an optically thin haze above an
optically thick cloud extending downward from the 300 mb level. The phase
function is derived for the cloud. Structure I represents our best estimate
of the true vertical structure for the South Tropical Zone and northern
component of the South Equatorial Belt derived from models which fit the
polarization and photometry in methane bands. Structure II is a single
optically thick cloud including no haze or molecular scattering. Because the
forward peaks of the phase functions are not constrained by our data, we have
not normalized each phase function to the same constant in Figs. 4 through 11.
Instead we have multiplied each by a factor which allows easy comparison of
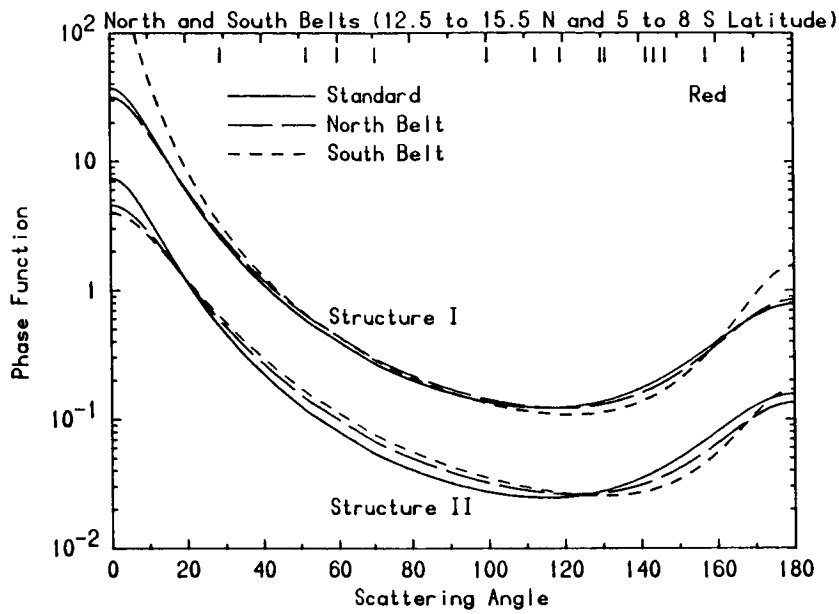the shapes over the range of scattering angles for which we have observations.

Figure 4. The best-fitting phase functions for
a northern belt and a southern belt are similar
in shape in red light. The differences are less
if Structure I, thought to be closer to the true
structure, is used. Vertical bars at the top
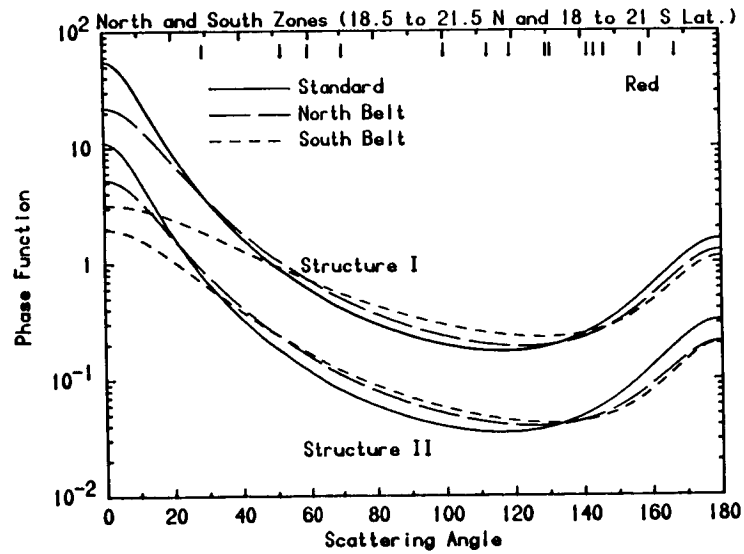show the scattering angles of the observations.

Figure 5. The best-fitting phase functions for
a northern zone and a southern zone have similar
shapes, and differ only slightly form the stand-
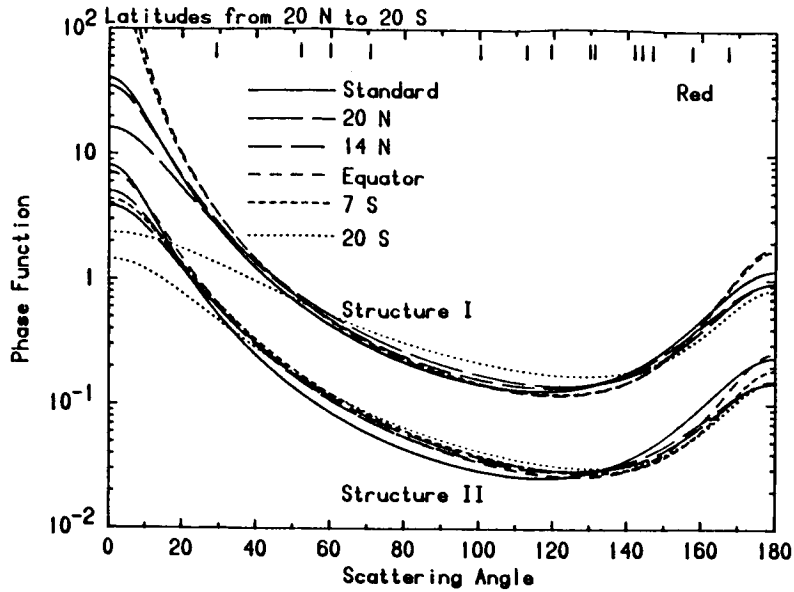ard zone phase function.

Figure 6. Best-fitting phase functions from six tropical latitudes are all similar in shape in red light. Belts are similar to zones.
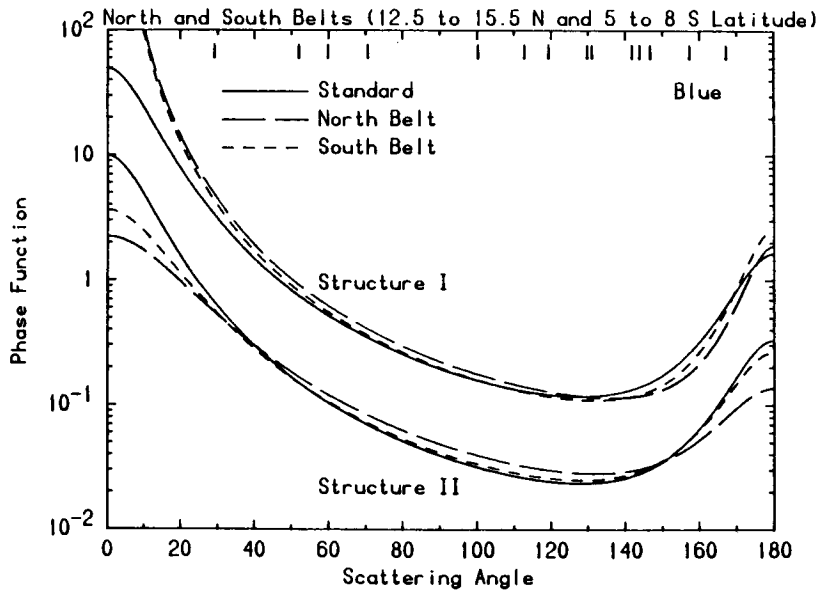

Figure 7. The same belts compared in Fig. 4 in red light are compared here in blue light. The phase functions are again similar in shape to each other and to the standard phase function.
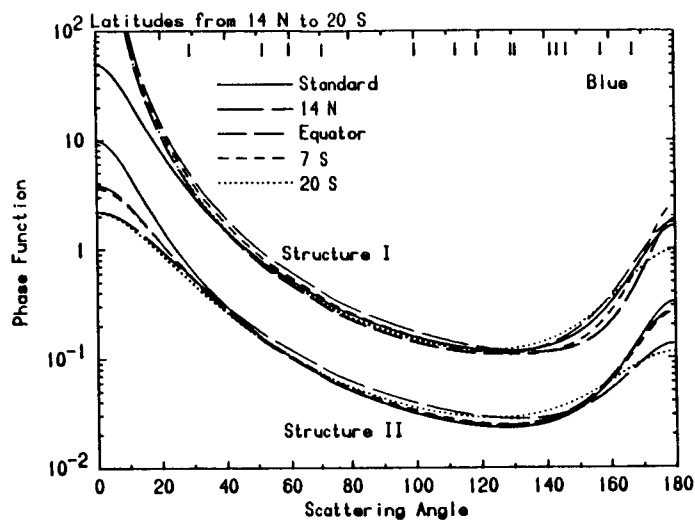
88

Figure 8. Best-fitting phase functions from
five tropical latitudes are even more similar
in blue light than in red light. Hemispheric
and albedo differences have little effect on
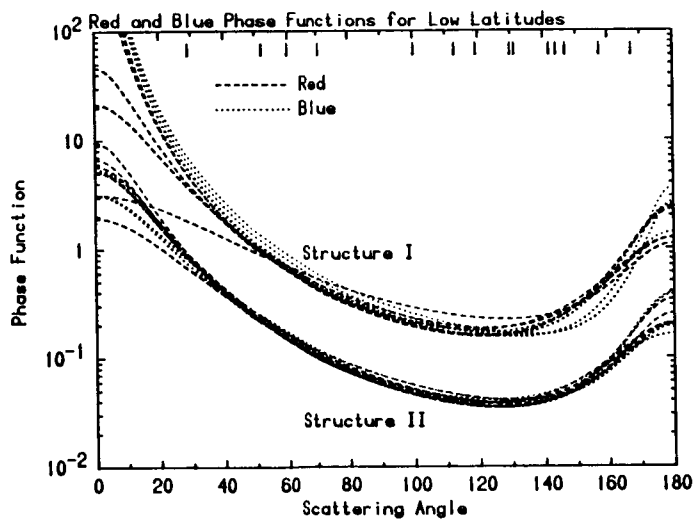single scattering phase function.

Figure 9. Phase functions derived in the red
and blue are compared for latitudes between 20
deg N and 20 deg S. For Structure I models the
blue phase functions are higher at intermediate
angles and have sharper backward peaks, but even
this marginally significant difference disap-
pears for Structure II models.

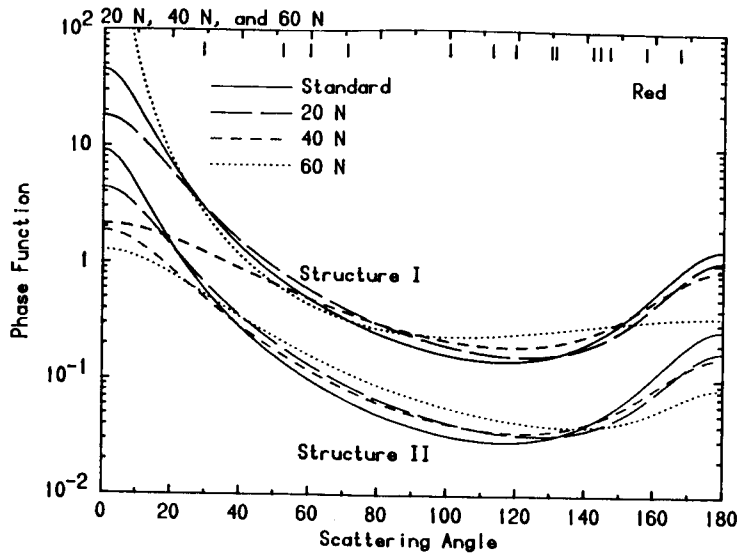Figure 10. A comparison of three regions shows the latitudinal dependence of the derived phase functions. The particles have significantly different phase functions at 60 deg N.
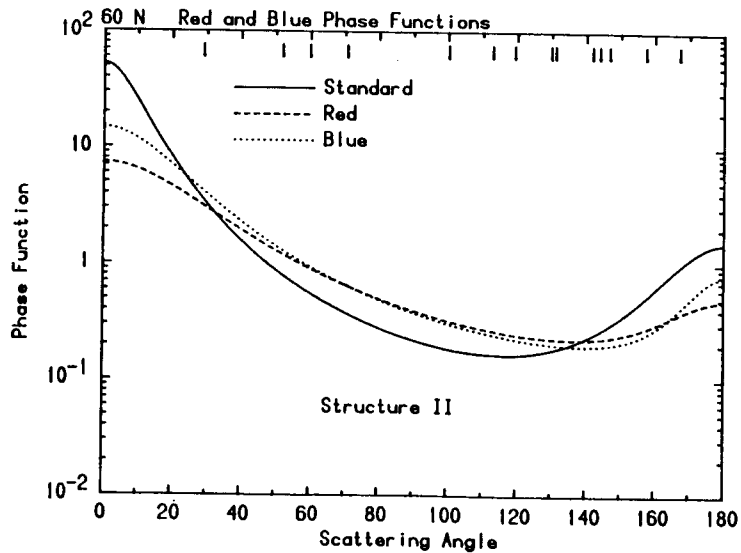

Figure 11. The phase function at 60 deg N has a different shape from the standard in both colors. The backward peak is steeper in blue than in red light, suggesting the presence of smaller particles at high latitudes than at low latitudes.

Figure 4 compares the phase functions for two belts in red light in the north
and south hemispheres. Figure 5 is a similar comparison for two zones. In
Figs. 4 through 11 the "standard" phase function derived by Tomasko *et al.*
(1978) is included for comparison. Figure 6 compares six tropical latitudes.
All of these phase functions are similar to each other and to the standard
phase function. The most significant difference occurs at 20 deg S where the
phase function is flatter and at the equator and 7 deg S where the backward
peak is more pronounced. The difference between the phase functions is
marginally significant. The dependence on vertical structure is small. At
intermediate scattering angles the phase functions derived using Structure II
are 10-20 percent higher than those from Structure I. At large scattering
angles this trend is reversed.

Similar comparisons in blue light are shown in Figs. 7 and 8. The phase func-
tions of these low latitude regions appear even more alike in blue light than
in red. The dependence on vertical structure is less also, a surprising
result considering the larger difference in optical properties in the blue
between structures resulting from an increase in optical depth from molecular
scattering.

The red and blue phase functions at low latitudes are compared in Fig. 9.
For Structure II no significant differences are evident. For Structure I the
blue phase functions have a steeper backward peak and a tendency to cross the
red phase functions from above to below as the scattering angle increases
through intermediate angles. To within our ability to determine the phase
functions using double Henyey-Greenstein functions, those at low latitudes
are all well represented by the standard phase functions of Tomasko *et al.*
(1978). The lack of dependence on the color of light is indicative of
particles large compared to the wavelength.

The phase functions are shown over a wider range of latitudes in Fig. 10. At
60 deg N the phase function is markedly different, being much flatter than
those at lower latitudes. This behavior is weakly indicated at 40 deg N also,
suggesting a progressive flattening of the function toward higher latitudes
beginning somewhere near 40 deg N. Smith and Tomasko (1984) found that the
polarization of Jupiter at large phase angles also showed a strong gradient
beginning near this latitude. Evidence for an increase in the optical thick-
ness of haze above the clouds at this latitude was also found by Tomasko and
Karkoschka. These studies together with Fig. 10 suggest the beginning of a
progressive change (with latitude) in the nature of scatterers. Figure 11
shows the phase functions derived at 60 deg N for red and blue light. The
flattening of the functions suggests that the scatterers may be smaller than
at lower latitudes. In the size range of a few tenths of micrometers the
change in the phase function from red to blue becomes predictable. The
particles appear smaller (in terms of wavelengths) to the red light, produc-
ing a phase function with molecular scattering-like tendencies. This effect
is diminished in blue light, in agreement with Fig. 11.

For those who need to use a phase function for radiative transfer modeling,
we recommend the double Henyey-Greenstein parameters given in Table 1. For
latitudes less than 40 deg the values are those of Tomasko *et al.* (1978).

We have shown that they apply over a broad range of latitudes. These parameters apply to a model with vertical Structure I, which includes a top haze layer of optical depth 0.25 over a molecular scattering optical depth of 0.04 in the red. In the blue the top layer is molecular scattering with optical depth 0.03 over a haze with optical depth 0.125 over another molecular scattering layer with optical depth 0.05. These layers are above the cloud, which begins at a pressure near 300 mb. The haze has a single Henyey-Greenstein phase function with g = 0.75. Its single scattering albedo is 0.95 in the red and 0.995 in the blue. At latitudes larger than 40 deg the haze is thought to be considerably thicker, and a simple optically thick cloud may be a better description of the vertical structure for the purpose of extracting phase functions. The parameters listed are from our solution at 60 deg N using Structure II. For all these latitudes the detailed nature of the forward peak at scattering angles less than 30° may differ from the given phase functions because we have no data to constrain it.

Table 1

Recommended Double Henyey-Greenstein Parameters

	Blue				Red			
	f	g_1	g_2	ω	f	g_1	g_2	ω
Latitudes < 40 deg*								
Belts	0.969	0.8	−0.8	0.97	0.938	0.8	−0.65	0.991
Zones	0.969	0.8	−0.8	0.995	0.938	0.8	−0.7	0.997
Latitudes > 40 deg	0.984	0.65	−0.78	0.988	0.976	0.57	−0.67	0.997

*From Tomasko et al. (1978)

To summarize, for scattering angles at which we are able to constrain the phase functions: (1) In red light at |latitude|<40 deg, belts, zones, and the equatorial region have similar phase functions. (2) This statement is also true for blue light. (3) Red and blue phase functions are similar, indicating the tropospheric cloud particles are large compared to either wavelength. (4) All phase functions derived for low latitudes are in good agreement with those found by Tomasko et al. (1978). (5) At latitudes larger than 40 deg N, the phase functions have less backward peak than at lower latitudes and show a significant difference between red and blue. This suggests the particles are small enough to show a wavelength dependence between 0.44 μm and 0.64 μm. We believe this is due to a thicker (probably photochemical) haze. This interpretation is supported by observations of the polarization and by ultraviolet photometry.

REFERENCES

Orton, G. S. (1975). Spatially resolved absolute spectral reflectivity of Jupiter: 3390-8400 Å. *Icarus* <u>26</u>, 159-174.

Smith, P. H., and M. G. Tomasko (1984). Photometry and polarimetry of Jupiter at large phase angles. II. Polarimetry of the South Tropical Zone, South Equatorial Belt, and the polar regions from the Pioneer 10 and 11 missions. *Icarus* <u>58</u>, 35-73.

Tomasko, M. G., E. Karkoschka, and S. Martinek (1986). Observations of the limb darkening of Jupiter at ultraviolet wavelengths and constraints on the properties and distribution of stratospheric aerosols. *Icarus* <u>65</u>, 218-243.

Tomasko, M. G., R. A. West, and N. D. Castillo (1978). Photometry and polarimetry of Jupiter at large phase angles. I. Analysis of imaging data of a prominent belt and a zone from Pioneer 10. *Icarus* <u>33</u>, 558-592.